

## Supplementary Information

### **Finely Modulated Asymmetric Nonfullerene Acceptor Enabling Simultaneously Improved Voltage and Current for Efficient Organic Solar Cells**

*Huanhuan Gao,<sup>a,b</sup> Xiangjian Wan,<sup>b</sup> Ziyi Xuan,<sup>c</sup> Wei Ma,<sup>c\*</sup> Jingming Xin,<sup>c</sup> Chenxi Li<sup>b</sup> and Yongsheng Chen<sup>b\*</sup>*

*<sup>a</sup> School of Materials Science and Engineering, Xian Shiyou University, Xi'an 710065, China.*

*<sup>b</sup> Key Laboratory of Functional Polymer Materials, College of Chemistry, Renewable Energy Conversion and Storage Center (RECAST), Nankai University, Tianjin 300071, China.*

*<sup>c</sup> State Key Laboratory for Mechanical Behavior of Materials, Xi'an Jiaotong University Xi'an 710049, China.*

#### Content

1. Measurements and Instruments
2. Materials synthesis and characterization
3. Fabrication of OSCs
4. Figures and Tables
5. NMR and HR-MS Spectra

## 1. Measurements and Instruments

The  $^1\text{H}$  and  $^{13}\text{C}$  nuclear magnetic resonance (NMR) spectra were taken on a Bruker AV400 Spectrometer. Matrix assisted laser desorption/ionization time-of-flight (MALDI-TOF) mass spectrometry were performed on a Bruker Autoflex III instrument. The HR-MS data were recorded on Varian 7.0T FT-MS. UV-vis spectra were obtained with a JASCO V-570 spectrophotometer. Cyclic voltammetry (CV) experiments were performed with a LK98B II Microcomputer-based Electrochemical Analyzer in  $\text{CH}_3\text{CN}$  solutions. All CV measurements were carried out at room temperature with a conventional three-electrode configuration employing a glassy carbon electrode as the working electrode, a saturated calomel electrode (SCE) as the reference electrode, and a Pt wire as the counter electrode. Tetrabutylammonium phosphorus hexafluoride ( $n\text{-Bu}_4\text{NPF}_6$ , 0.1 M) in  $\text{CH}_3\text{CN}$  was used as the supporting electrolyte, and the scan rate was  $50 \text{ mV s}^{-1}$ . The highest occupied molecular orbital (HOMO) and lowest unoccupied molecular orbital (LUMO) energy levels were calculated from the onset oxidation potential and the onset reduction potential, using the equation  $E_{\text{HOMO}} = - (4.80 + E_{\text{ox}}^{\text{onset}})$ ,  $E_{\text{LUMO}} = - (4.80 + E_{\text{red}}^{\text{onset}})$ .

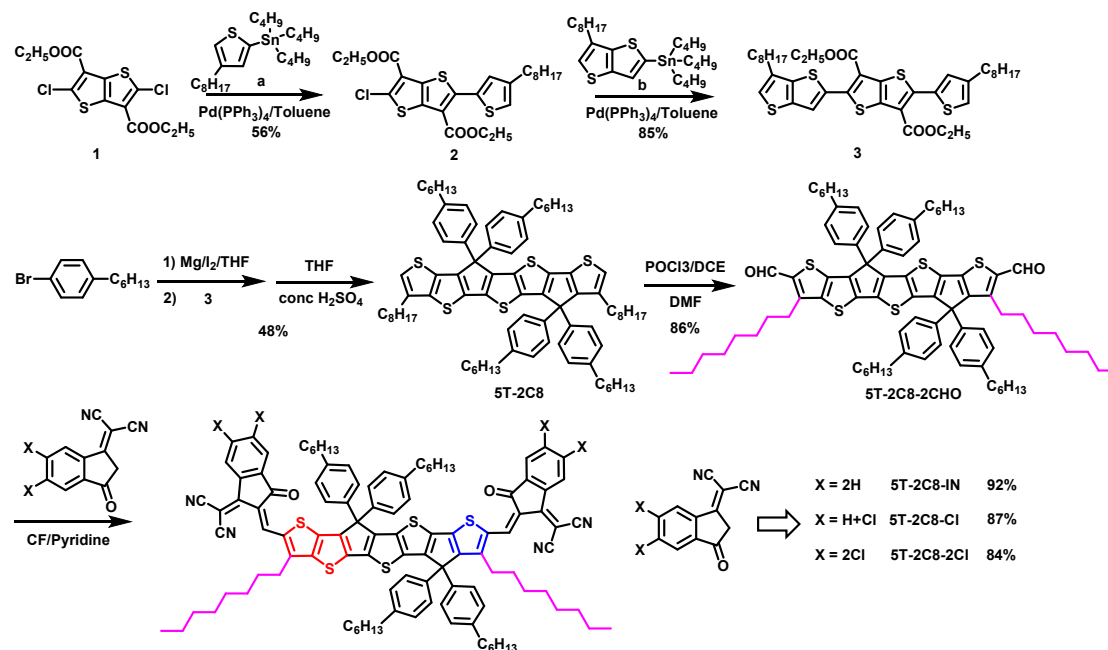
Atomic force microscope (AFM) investigation was performed using Bruker MultiMode 8 in tapping mode. The current density-voltage ( $J$ - $V$ ) characteristics of photovoltaic devices were obtained using a Keithley 2400 source-measure unit. The current density-voltage ( $J$ - $V$ ) characteristics of photovoltaic devices were obtained using a Keithley 2400 source-measure unit. The photocurrent was measured under illumination simulated  $100 \text{ mW cm}^{-2}$  AM1.5G irradiation using a SAN-EI XES-70S1 solar simulator, calibrated with a standard Si solar cell (Enli Technology Co., Ltd., Taiwan, and calibrated report can be traced to NREL). The external quantum efficiency (EQE) spectrum was measured using a QE-R Solar Cell Spectral Response Measurement System (Enli Technology Co., Ltd., Taiwan). The hole and electron mobility were measured using the space charge limited current (SCLC) method, employing a diode configuration of ITO/PEDOT:PSS/active layer/Au for hole and glass/ITO/ZnO/active layer/Al for electron by taking the dark current density in the

range of 0-8 V and fitting the results to a space charge limited form, where SCLC is described by:

$$J = \frac{9\varepsilon_0\varepsilon_r\mu_0V^2}{8L^3}$$

where  $J$  is the current density,  $L$  is the film thickness of the active layer,  $\mu$  is the hole or electron mobility,  $\varepsilon_r$  is the relative dielectric constant of the transport medium,  $\varepsilon_0$  is the permittivity of free space ( $8.85 \times 10^{-12}$  F m<sup>-1</sup>),  $V$  ( $= V_{\text{appl}} - V_{\text{bi}}$ ) is the internal voltage in the device, where  $V_{\text{appl}}$  is the applied voltage to the device and  $V_{\text{bi}}$  is the built-in voltage due to the relative work function difference of the two electrodes.

## 2. Materials synthesis and characterization



**Scheme 1.** The synthetic routes of 5T-2C8-IN, 5T-2C8-Cl, 5T-2C8-2Cl and 6T-2C8-2Cl.

All reactions and manipulations were carried out using the standard Schlenk techniques. All the raw materials were purchased from commercial suppliers and used without further purification unless indicated otherwise. PBDB-TF (PM6) was purchased from Solarmer.

**Compound 2:** Under the atmosphere of argon, compound 1 (Thieno[3,2-b]thiophene-

3,6-dicarboxylic acid, 2,5-dichloro-3,6-diethyl ester), 1 g (2.83 mmol), compound **a**, 1.37 g (2.83 mmol) and Ph(PPh<sub>3</sub>)<sub>4</sub>, 163 mg (0.142 mmol) were added into 100 mL two-neck flask and degassed with argon three times. Then 25 mL anhydrous toluene was injected into the reaction system and stirred at 100 °C for 3 hours. The reaction solution was cooled to room temperature and poured into 100 mL anhydrous methanol, then filtered and washed with a petroleum ether (PE) and methanol. The crude product was purified by column chromatography using CH<sub>2</sub>Cl<sub>2</sub>/PE (1:2) as the eluent to give compound **2** as a pale yellow solid (56%). <sup>1</sup>H NMR (400 MHz, CDCl<sub>3</sub>) δ 7.42 (d, *J* = 5.2 Hz, 1H), 7.27 (d, *J* = 1.2 Hz, 1H), 4.45 – 4.43 (m, 4H), 2.73 – 2.67 (m, 2H), 1.74 – 1.64 (m, 3H), 1.48 – 1.43 (m, 10H), 1.23 – 1.19 (m, 6H), 0.84 (t, *J* = 7.0 Hz, 3H). MS (MALDI-TOF): calcd for C<sub>24</sub>H<sub>29</sub>ClO<sub>4</sub>S<sub>3</sub> [M<sup>+</sup>], 512.092, found 512.097.

**Compound 3:** compound **2**, 500 mg (0.974 mmol), compound **b**, 633 mg (1.169 mmol) and Ph(PPh<sub>3</sub>)<sub>4</sub>, 57 mg (0.049 mmol) were added into a 100 mL two neck round-bottom flask and degassed with argon three times. Then 15 mL anhydrous toluene was injected into the reaction system and stirred at 110 °C overnight. The reaction solution was cooled to room temperature and poured into 100 mL anhydrous methanol, then filtered and washed with a petroleum ether, ethyl acetate and methanol. The crude product was purified by column chromatography using CH<sub>2</sub>Cl<sub>2</sub>/PE (1:1) as the eluent to give compound **3** as a yellow solid (83%). <sup>1</sup>H NMR (400 MHz, CDCl<sub>3</sub>) δ 7.45 – 7.38 (m, 2H), 7.10 – 7.03 (m, 2H), 4.44 – 4.36 (m, 4H), 2.72 – 2.55 (m, 4H), 1.57 – 1.55 (m, 4H), 1.31 – 1.27 (m, 22H), 0.90 – 0.88 (m, 6H). MS (MALDI-TOF): calcd for C<sub>30</sub>H<sub>32</sub>O<sub>4</sub>S<sub>5</sub> [M<sup>+</sup>], 616.090, found 616.083.

**Compound 5T-2C8:** Under the atmosphere of argon, 1-bromo-4-hexylbenzene, 1.41 g (5.846 mmol), in anhydrous THF (30 mL) and then 2.6 mL n-BuLi (2.4 M) was added into the reaction system dropwise in -78 °C. The reaction was stirred at -78 °C for 1 h. Compound **3**, 600 mg (0.973 mmol) was added into the system quickly, and the reaction was stirred at room temperature for another 12 h. The reaction solution was quenched with water (100mL) and washed brine (300 mL) for three times and dried over anhydrous Na<sub>2</sub>SO<sub>4</sub>. The solvent was removed under vacuum. The crude product was dissolved in THF 30 mL and 0.5 mL conc. H<sub>2</sub>SO<sub>4</sub> was added as the catalyst. The reaction mixture was stirred at 75 °C for 2 h and quenched with 10 mL ice water and

washed with water for 4 times. The mixture was extracted with chloroform (100mL). The organic phase was separated and dried with anhydrous Na<sub>2</sub>SO<sub>4</sub>. The solvent was removed under vacuum, and the crude product was purified by column chromatography using PE as the eluent to give compound **5T-2C8** as a yellow solid (48%). <sup>1</sup>H NMR (400 MHz, CDCl<sub>3</sub>) δ 7.52 – 7.48 (m, 2H), 7.09 – 7.08 (m, 8H), 7.07 – 7.06 (m, 8H), 6.77 (s, 2H), 2.56 – 2.53 (m, 12H), 1.76 – 1.69 (m, 12H), 1.28 – 1.26 (m, 44H), 0.89 – 0.89 (m, 18H). MS (MALDI-TOF): calcd for C<sub>82</sub>H<sub>104</sub>S<sub>5</sub> [M<sup>+</sup>], 1248.674, found 1248.662.

**Compound 5T-2C8-2CHO:** Under the atmosphere of argon, anhydrous N,N-dimethylformamide (6 mL) was added into a two neck round flask. Then anhydrous phosphorus oxychloride (POCl<sub>3</sub>) (273 μL) was injected into the reaction system drop by drop under the ice-water bath. The reaction was stirred under 0 °C for 30 minutes. After that, the ice-water bath was removed and stirred in the room temperature for another 3 hours to gain the Vilsmerier reagent. Then, the Vilsmerier reagent was added into a 1,2-dichloroethane (80 mL) solution of compound **5T**, 600 mg (0.585 mmol). The above reaction mixture was stirred at room atmosphere for 1 h and then 70 °C over night. 30 mL saturated sodium acetate solution was added slowly to quench the reaction. The above mixture solution was washed with water for three times. The organic phase was separated and dried over anhydrous Na<sub>2</sub>SO<sub>4</sub>. The solvent was removed under vacuum, and the crude product was purified by column chromatography using CH<sub>2</sub>Cl<sub>2</sub>/PE (1:1) as the eluent to give compound **5T-2CHO** as an orange solid (86%). <sup>1</sup>H NMR (400 MHz, CDCl<sub>3</sub>) δ 9.99 (s, 1H), 9.88 (s, 1H), 7.20 – 7.11 (m, 8H), 7.10 – 7.08 (m, 8H), 3.05 (t, *J* = 7.7 Hz, 2H), 2.72 – 2.66 (m, 2H), 2.59 – 2.52 (m, 8H), 1.64 – 1.51 (m, 12H), 1.36 – 1.22 (m, 44H), 0.88 – 0.84 (m, 18H). MS (MALDI-TOF): calcd for C<sub>84</sub>H<sub>104</sub>O<sub>2</sub>S<sub>5</sub> [M<sup>+</sup>], 1304.6640, found 1304.6690.

**5T-2C8-IN:** A mixture of compound **5T-2C8-2CHO**, 150 mg (0.115 mmol), 2-(2,3-dihydro-3-oxo-1H-inden-1-ylidene) 67 mg (0.345 mmol) in chloroform 20 mL and 0.5 mL pyridine was added as the catalyst under argon atmosphere. The reaction was stirred at room temperature for 12 hours under dark. The organic phase was washed with water for three times and dried over anhydrous Na<sub>2</sub>SO<sub>4</sub>. The solvent was removed under vacuum, and the crude product was purified by column chromatography using CF/PE (1:1) as the eluent to give the crude product, which was purified with further

recrystallization using CF/methanol to obtain compound **5T-2C8-IN** as a dark green solid (92%). <sup>1</sup>H NMR (400 MHz, CDCl<sub>3</sub>) δ 9.04 (s, 1H), 8.95 (s, 1H), 8.70 (t, J = 7.5 Hz, 2H), 7.93 – 7.88 (m, 2H), 7.77 – 7.69 (m, 4H), 7.22 – 7.14 (m, 16H), 3.13 (t, J = 7.7 Hz, 2H), 2.81 – 2.74 (m, 2H), 2.62 – 2.56 (m, 8H), 1.81 – 1.75 (m, 2H), 1.64 – 1.58 (m, 8H), 1.54 – 1.45 (m, 4H), 1.35 – 1.28 (m, 32H), 1.19 – 1.12 (m, 6H), 1.02 – 0.97 (m, 2H), 0.90 – 0.86 (m, 18H), 0.68 – 0.62 (m, 2H). MS (MALDI-TOF): calcd for C<sub>108</sub>H<sub>112</sub>N<sub>4</sub>O<sub>2</sub>S<sub>5</sub> [M<sup>+</sup>], 1656.7389, found 1656.7449.

**5T-2C8-Cl**: The synthetic process is similar with the general procedure of 5T-2C8-IN, 5T-2C8-Cl was obtained as a dark green solid (87%). <sup>1</sup>H NMR (400 MHz, CDCl<sub>3</sub>) δ 9.01 (s, 1H), 8.92 (s, 1H), 8.66 – 8.57 (m, 2H), 7.84 – 7.77 (m, 2H), 7.66 (t, J = 7.5 Hz, 2H), 7.24 – 7.09 (m, 16H), 3.14 – 3.06 (m, 2H), 2.79 – 2.71 (m, 2H), 2.64 – 2.52 (m, 8H), 1.79 – 1.71 (m, 2H), 1.66 – 1.56 (m, 8H), 1.54 (s, 2H), 1.46 – 1.42 (m, 2H), 1.37 – 1.24 (m, 32H), 1.19 – 1.08 (m, 6H), 0.99 – 0.94 (m, 2H), 0.87 (t, J = 5.9 Hz, 18H), 0.67 – 0.58 (m, 2H). MS (MALDI-TOF): calcd for C<sub>108</sub>H<sub>110</sub>Cl<sub>2</sub>N<sub>4</sub>O<sub>2</sub>S<sub>5</sub> [M<sup>+</sup>], 1724.6609, found 1724.6680.

**5T-2C8-2Cl**: Following the general procedure of 5T-2C8-IN, 5T-2C8-2Cl was obtained as a dark green solid (84%). <sup>1</sup>H NMR (400 MHz, CDCl<sub>3</sub>) δ 9.04 (s, 1H), 8.94 (s, 1H), 8.77 (d, J = 7.5 Hz, 2H), 7.93 (d, J = 12.8 Hz, 2H), 7.22 – 7.14 (m, 16H), 3.12 (t, J = 7.7 Hz, 2H), 2.81 – 2.73 (m, 2H), 2.60 (dd, J = 15.1, 5.6 Hz, 8H), 1.81 – 1.74 (m, 2H), 1.65 – 1.58 (m, 8H), 1.49 – 1.44 (m, 2H), 1.37 – 1.26 (m, 34H), 1.20 – 1.10 (m, 6H), 1.02 – 0.96 (m, 2H), 0.91 – 0.86 (m, 18H), 0.64 (s, 2H). <sup>13</sup>C NMR (101 MHz, CDCl<sub>3</sub>) δ 186.28, 186.08, 158.91, 158.84, 157.98, 157.55, 157.32, 154.92, 153.30, 152.85, 149.41, 148.72, 145.56, 145.00, 143.15, 141.45, 140.90, 139.51, 139.41, 139.06, 138.71, 136.91, 136.52, 136.18, 136.02, 135.60, 135.34, 135.14, 135.02, 129.21, 128.96, 128.02, 127.70, 126.82, 126.70, 125.00, 124.79, 119.90, 118.51, 115.29, 115.13, 114.98, 114.66, 68.32, 67.11, 62.71, 62.56, 35.64, 35.60, 31.90, 31.84, 31.69, 31.27, 31.19, 30.29, 29.74, 29.49, 29.35, 29.26, 29.19, 29.12, 22.68, 22.65, 22.59, 14.13, 14.10. MS (MALDI-TOF): calcd for C<sub>108</sub>H<sub>108</sub>Cl<sub>4</sub>N<sub>4</sub>O<sub>2</sub>S<sub>5</sub> [M<sup>+</sup>], 1792.5380, found 1792.5943.

**6T-2C8-2Cl**: A mixture of compound **6T-2C8-2CHO**, 200 mg (0.147 mmol), 2-(5,6-dichloro-2,3-dihydro-3-oxo-1H-inden-1-ylidene) 116 mg (0.441 mmol) in chloroform 20 mL and 0.6 mL pyridine was added as the catalyst under argon atmosphere. The

reaction was stirred at room temperature for 12 hours under dark. The organic phase was washed with water for three times and dried over anhydrous  $\text{Na}_2\text{SO}_4$ . The solvent was removed under vacuum, and the crude product was purified by column chromatography using CF/PE (1:1) as the eluent to give the crude product and then purified with further recrystallization using CF/methanol to obtain compound **6T-2C8-2Cl** as a dark green solid (89%).  $^1\text{H}$  NMR (400 MHz,  $\text{CDCl}_3$ )  $\delta$  9.01 (s, 2H), 8.75 (s, 2H), 7.91 (s, 2H), 7.20 – 7.15 (m, 16H), 3.11 (t,  $J = 7.6$  Hz, 4H), 2.59 – 2.53 (m, 8H), 1.80 – 1.72 (m, 4H), 1.61 – 1.58 (m, 4H), 1.48 – 1.42 (m, 4H), 1.34 – 1.24 (m, 44H), 0.90 – 0.83 (m, 18H).  $^{13}\text{C}$  NMR (101 MHz,  $\text{CDCl}_3$ )  $\delta$  186.12, 158.89, 153.45, 153.15, 149.47, 148.74, 145.86, 144.77, 143.05, 139.83, 139.29, 138.93, 138.74, 138.21, 136.70, 136.02, 135.55, 134.80, 129.17, 127.75, 126.79, 124.92, 119.52, 115.23, 114.76, 67.96, 62.62, 35.64, 31.85, 31.68, 31.20, 29.77, 29.36, 29.20, 29.14, 22.66, 22.58, 14.13, 14.09. MS (MALDI-TOF): calcd for  $\text{C}_{110}\text{H}_{108}\text{Cl}_4\text{N}_4\text{O}_2\text{S}_6$  [ $\text{M}^+$ ], 1848.5551, found 1848.57.

### 3 Fabrication of OSCs

The OSCs devices were fabricated using an inverted structure of ITO/ZnO/PFN-Br/active layers/MoOx/Ag. The indium tin oxide (ITO)-coated glass substrates were cleaned by ultrasonic treatment in detergent, deionized water, acetone, and isopropyl alcohol under ultrasonication for 15 min each and subsequently dried by a nitrogen blow. Subsequently, a 30 nm thick layer of ZnO was deposited by spin-coating a ZnO precursor solution on the top of the ITO glass substrates at 3000 rpm for 40 s. After being baked at 200 °C in air for 60 min, the ZnO-coated substrates were transferred into a nitrogen-filled glove box. ZnO film thickness is ~30 nm. In order to fine-tune the interfacial properties a thin film of PFN-Br was spin-coated on ZnO. Subsequently, the P6:NFA in chlorobenzene (CB) with DIO additive was spin-coated onto PFN-Br layer. MoOx (~6 nm) and Ag (~70 nm) was successively evaporated onto the active layer through a shadow mask (pressure ca.  $10^{-4}$  Pa). The effective area for the devices is 4  $\text{mm}^2$ .

### 4 Figures and tables

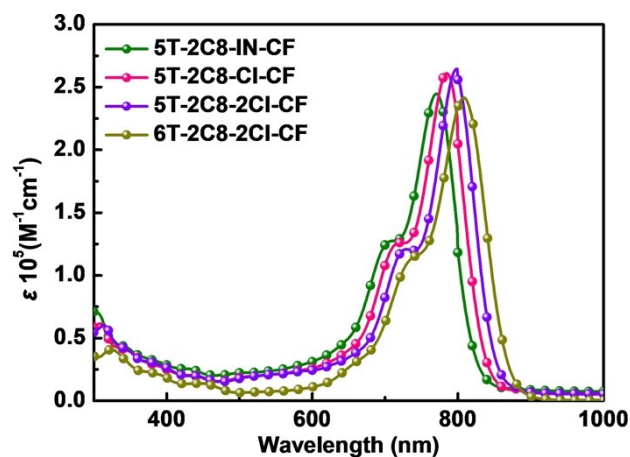


**Figure S1.** The UV-vis absorption spectra of 5T-2C8-IN, 5T-2C8-Cl and 5T-2C8-2Cl and 6T-2C8-2Cl in dilute chloroform.

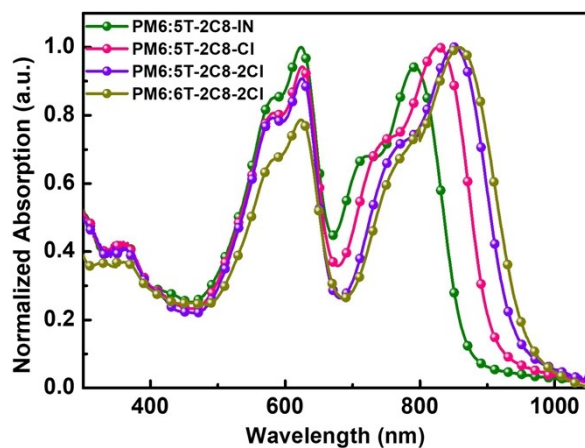


**Figure S2.** The UV-vis absorption spectra of 5T-2C8-IN, 5T-2C8-Cl and 5T-2C8-2Cl and 6T-2C8-2Cl based blend films in thin films.

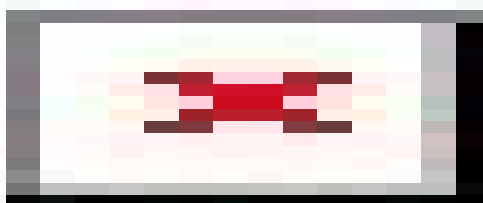


**Figure S3.** The optimized geometry conformation and its corresponding HOMO and LUMO energy levels electron cloud distribution of 6T-2C8-2Cl, 5T-2C8-2Cl, 5T-2C8-Cl and 5T-2C8-IN by DFT calculation.

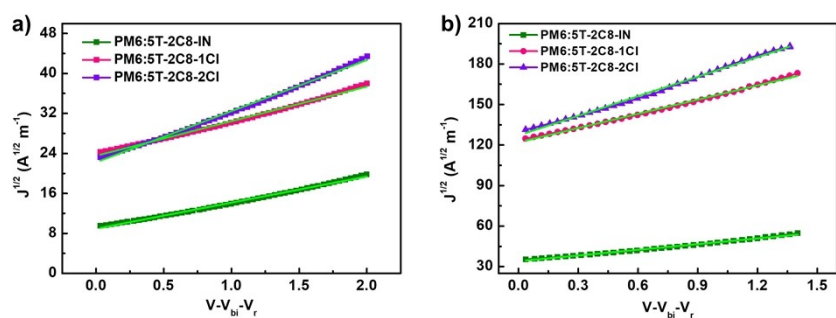


**Figure S4.** The electron (a) and hole (b) mobility of the optimized device, with film thickness of 119, 102, 96 and 105 nm for the 5T-2C8-IN, 5T-2C8-Cl and 5T-2C8-2Cl and 6T-2C8-2Cl based electron and hole devices, respectively.

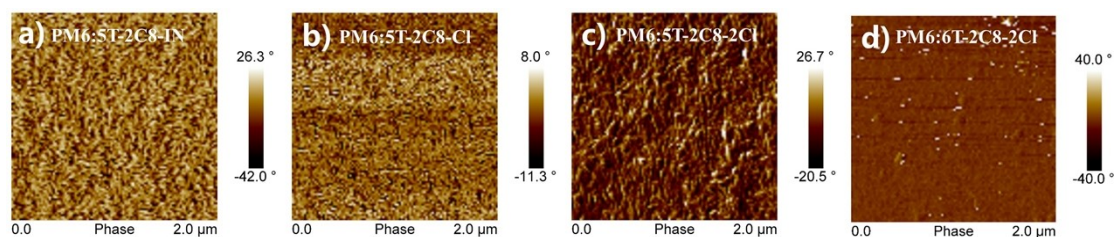


**Figure S5.** The corresponding phase image of PM6:5T-2C8-IN (a), PM6:5T-2C8-Cl (b), PM6:5T-2C8-2Cl (c) and PM6:6T-2C8-2Cl (d) blend film.

Table S1. Summarized of the photovoltaic performances with different donor/acceptor weight ratio for PM6:5T-2C8-IN based devices.

D:A	$V_{oc}$ (V)	$J_{sc}$ (mA cm <sup>-2</sup> )	FF	PCE (%)
1:0.8	0.979	10.22	0.47	4.70
1:1	0.967	9.88	0.50	4.77
1:1.2	0.965	9.18	0.50	4.43

Table S2. Summarized of the photovoltaic performances with different DIO additive (vol%) for PM6:5T-2C8-IN based devices.

DIO Additive	$V_{oc}$ (V)	$J_{sc}$ (mA cm <sup>-2</sup> )	FF	PCE (%)
0.4%	0.968	10.22	0.51	5.04
0.6%	0.969	10.33	0.52	5.21
0.8%	0.965	10.09	0.51	4.96

Table S3. Summarized of the photovoltaic performances with different TA treatment for PM6:5T-2C8-IN based devices.

Condition	$V_{oc}$ (V)	$J_{sc}$ (mA cm <sup>-2</sup> )	FF	PCE (%)
As cast	0.969	10.33	0.52	5.21
120 °C	0.923	10.03	0.46	4.26
140 °C	0.929	10.17	0.45	4.25
160 °C	0.923	11.33	0.51	5.33

Table S4. Summarized of the photovoltaic performances with different donor/acceptor weight ratio for PM6:5T-2C8-Cl based devices.

D:A	$V_{oc}$ (V)	$J_{sc}$ (mA cm <sup>-2</sup> )	FF	PCE (%)
1:0.8	0.896	17.51	0.54	8.47
1:1	0.892	17.80	0.55	8.73
1:1.2	0.888	17.41	0.55	8.50

Table S5. Summarized of the photovoltaic performances with different DIO additive (vol%) for PM6:5T-2C8-Cl based devices.

DIO Additive	$V_{oc}$ (V)	$J_{sc}$ (mA cm <sup>-2</sup> )	FF	PCE (%)
0.4%	0.886	18.35	0.58	9.43
0.6%	0.870	20.53	0.59	10.54
0.8%	0.871	19.78	0.59	10.16
1.0%	0.875	19.27	0.59	9.95

Table S6. Summarized of the photovoltaic performances with different TA treatment for PM6:5T-2C8-Cl based devices.

Condition	$V_{oc}$ (V)	$J_{sc}$ (mA cm <sup>-2</sup> )	FF	PCE (%)
As cast	0.870	20.53	0.59	10.54
120 °C	0.870	20.80	0.65	11.76
140 °C	0.868	21.23	0.65	11.98
160 °C	0.862	20.68	0.66	11.76

Table S7. Summarized of the photovoltaic performances with different donor/acceptor weight ratio for PM6:5T-2C8-2Cl based devices.

D:A	$V_{oc}$ (V)	$J_{sc}$ (mA cm <sup>-2</sup> )	FF	PCE (%)
1:0.8	0.834	21.74	0.52	9.43
1:1	0.831	22.24	0.52	9.61
1:1.2	0.823	21.63	0.52	9.26

Table S8. Summarized of the photovoltaic performances with different DIO additive (vol%) for PM6:5T-2C8-2Cl based devices.

DIO Additive	$V_{oc}$ (V)	$J_{sc}$ (mA cm <sup>-2</sup> )	FF	PCE (%)
0.4%	0.820	22.17	0.55	10.00
0.6%	0.818	22.79	0.57	10.63
0.8%	0.816	22.83	0.54	10.06
1.0%	0.817	22.89	0.53	9.91

Table S9. Summarized of the photovoltaic performances with different TA treatment for PM6:5T-2C8-2Cl based devices.

Condition	$V_{oc}$ (V)	$J_{sc}$ (mA cm <sup>-2</sup> )	FF	PCE (%)
As cast	0.818	22.79	0.57	10.63
120 °C	0.799	24.60	0.64	12.58
140 °C	0.802	24.97	0.65	13.02
160 °C	0.797	24.05	0.65	12.46

Table S10. Summarized of the photovoltaic performances with PCE10 as the polymer for PCE10:5T-2C8-IN/5T-2C8-Cl/5T-2C8-2Cl based devices under the optimized condition.

Devices	$V_{oc}$ (V)	$J_{sc}$ (mA cm <sup>-2</sup> )	FF	PCE (%)
PCE10:5T-2C8-IN	0.961	10.33	0.52	5.16
PCE10:5T-2C8-Cl	0.861	20.25	0.65	11.33
PCE10:5T-2C8-2Cl	0.800	23.82	0.65	12.39

Table S11. Summarized of the photovoltaic performances using conventional device structure of ITO/PEDOT:PSS/PM6:5T-2C8-2Cl/PDINO/Al under the optimized condition.

Devices	$V_{oc}$ (V)	$J_{sc}$ (mA cm <sup>-2</sup> )	FF	PCE (%)
PM6:5T-2C8-2Cl	0.803	23.20	0.65	12.20

## 5 NMR and HR-MS Spectra

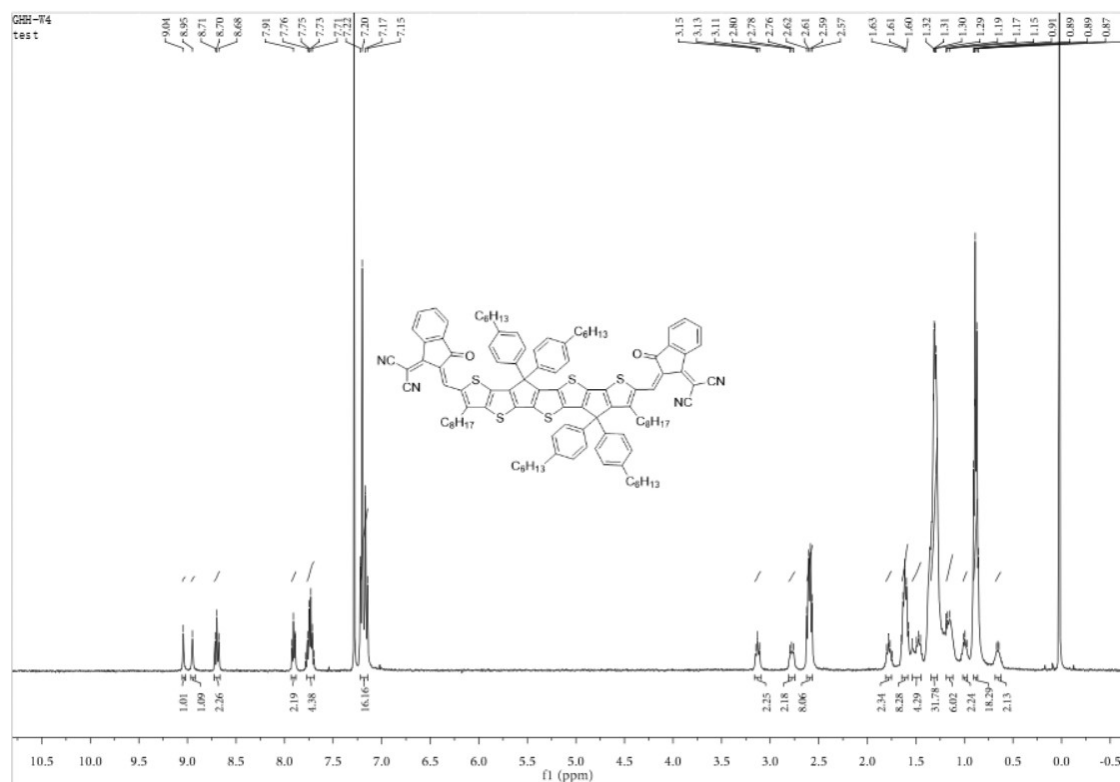


Fig. S6. <sup>1</sup>H NMR of compound 5T-2C8-IN in CDCl<sub>3</sub>.

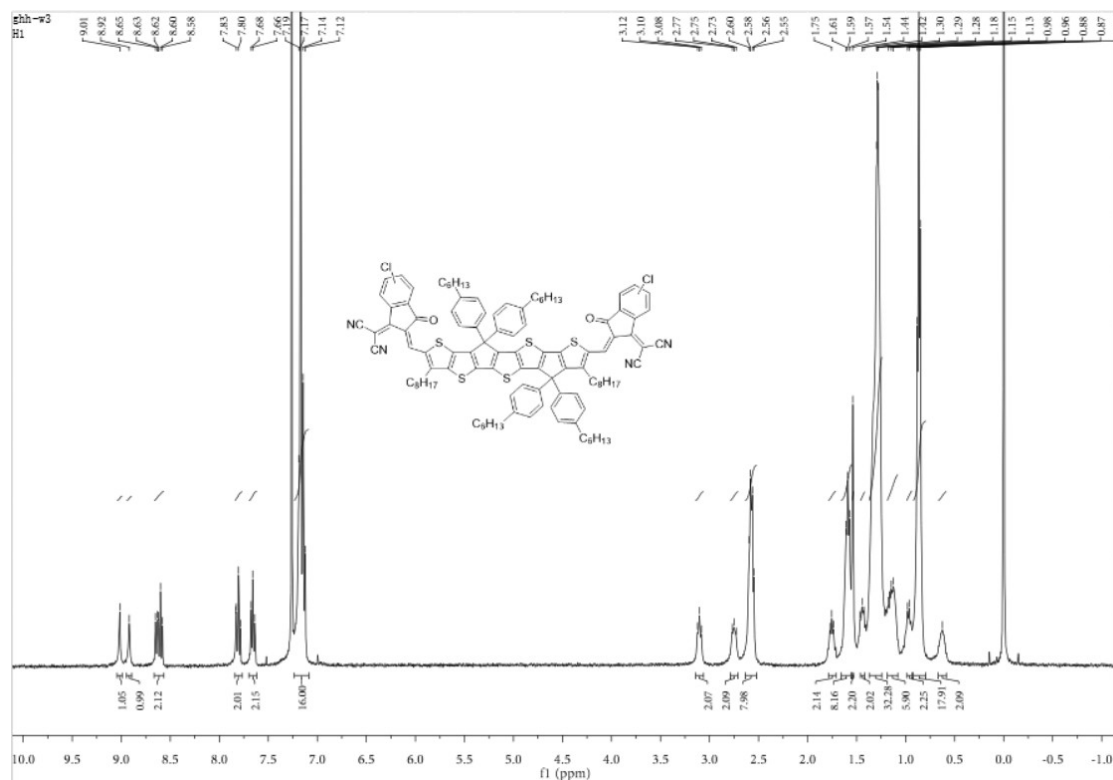


Fig. S7.  $^{13}\text{C}$  NMR of compound 5T-2C8-Cl in  $\text{CDCl}_3$ .

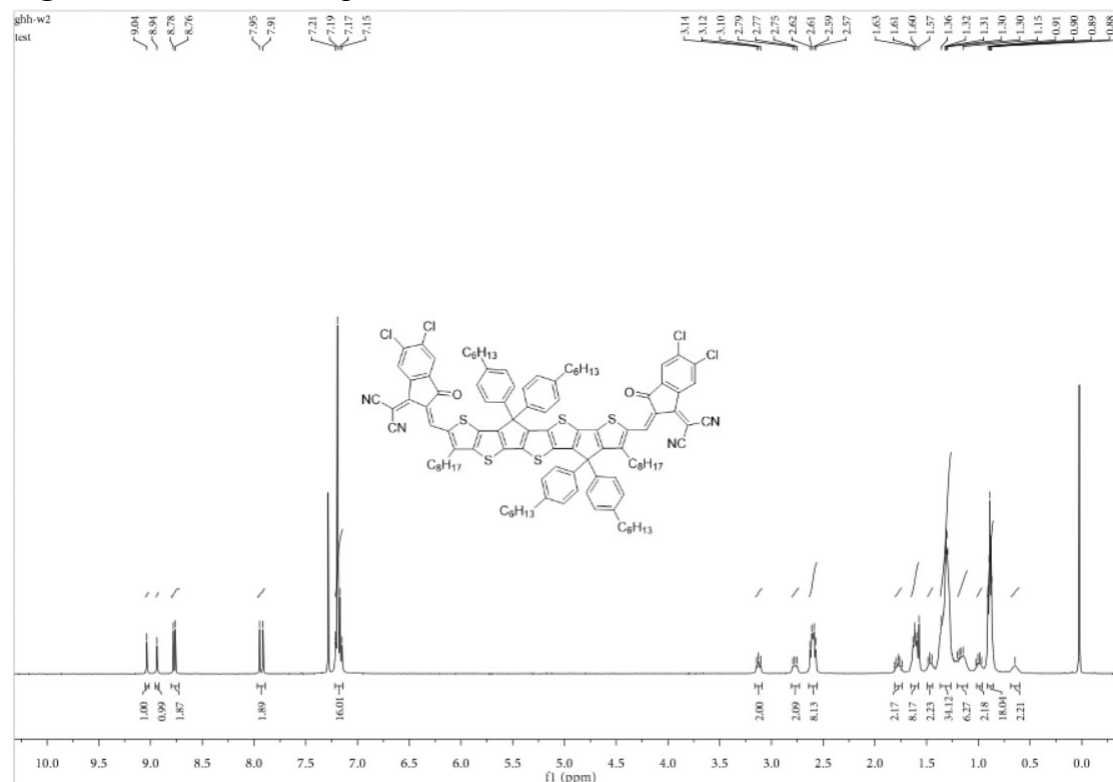
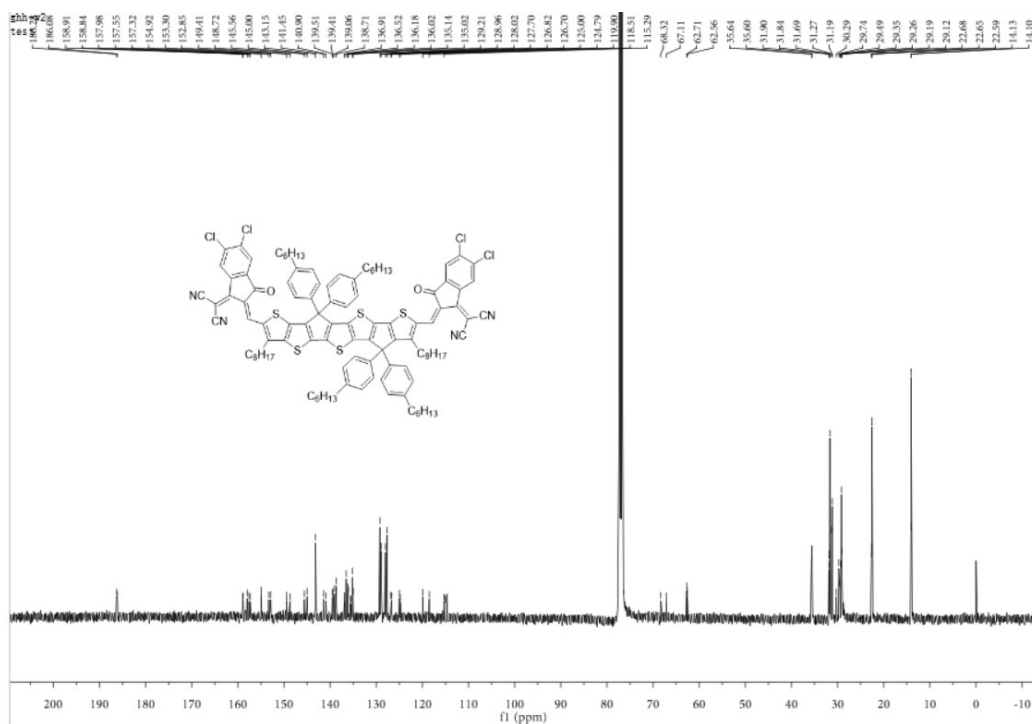
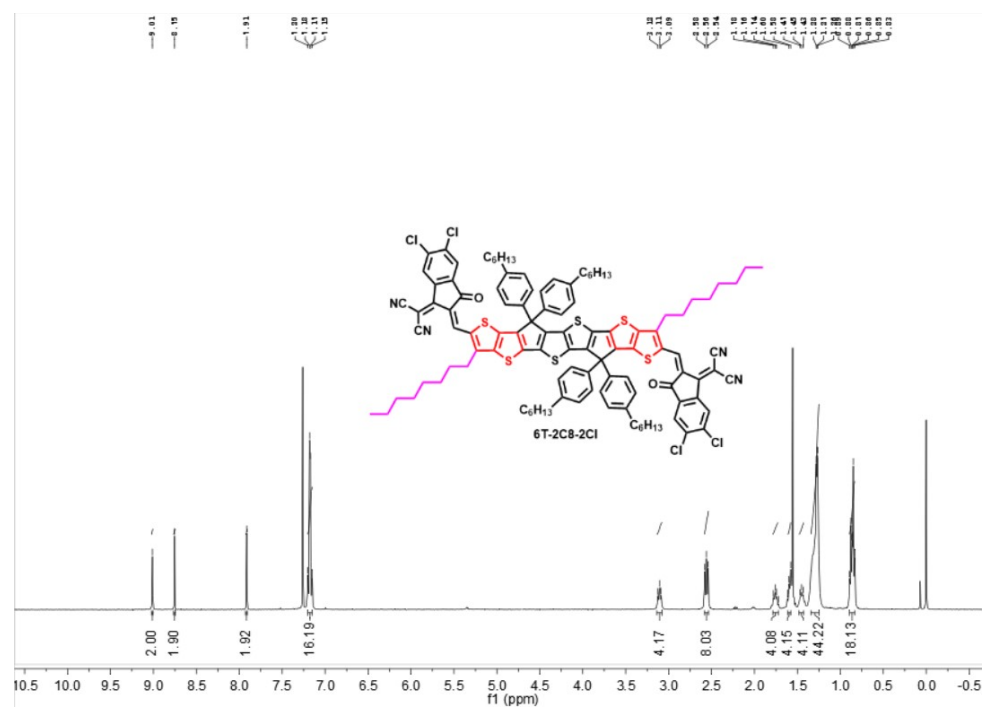


Fig. S8.  $^1\text{H}$  NMR of compound 5T-2C8-2Cl in  $\text{CDCl}_3$ .



**Fig. S9.**  $^{13}\text{C}$  NMR of compound 5T-2C8-2Cl in  $\text{CDCl}_3$ .



**Fig. S10.**  $^1\text{H}$  NMR of compound 6T-2C8-2Cl in  $\text{CDCl}_3$ .

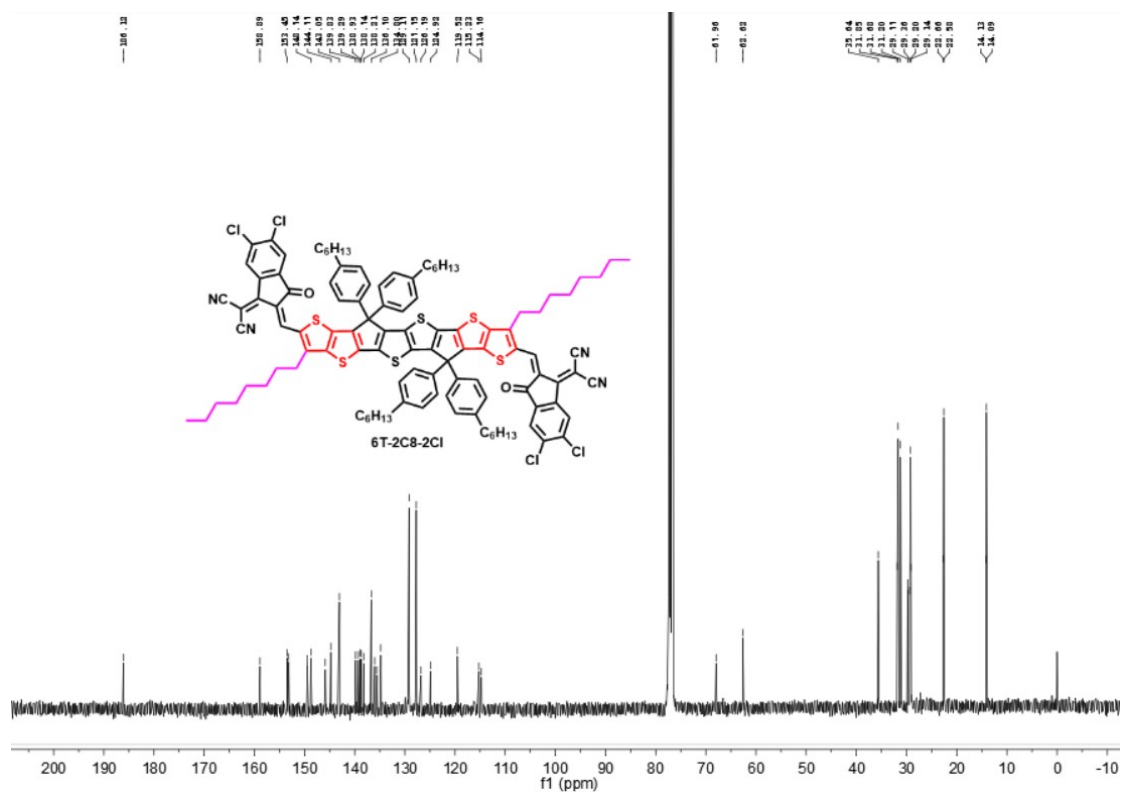
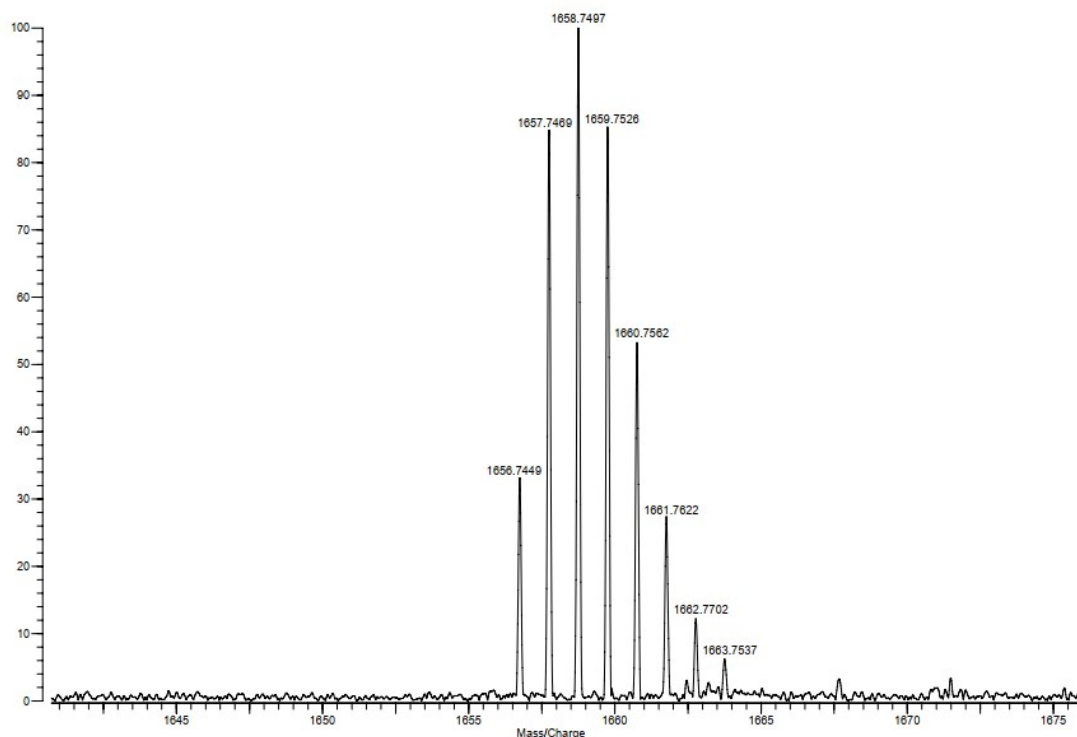
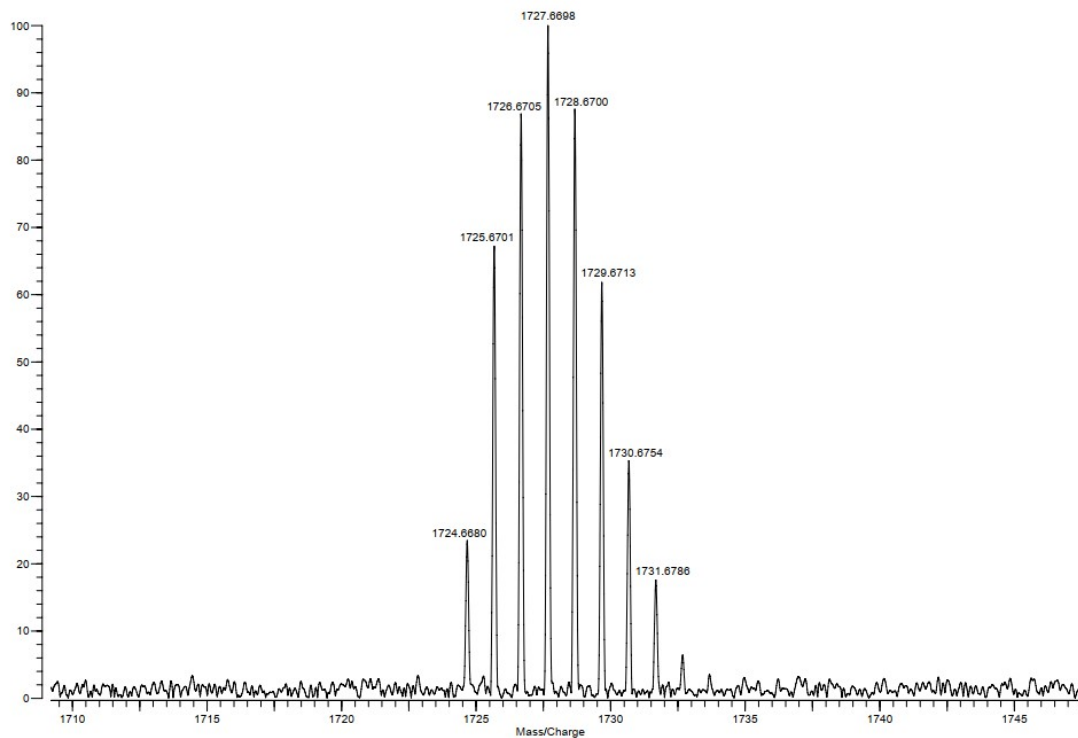


Fig. S11.  $^{13}\text{C}$  NMR of compound 6T-2C8-2Cl in  $\text{CDCl}_3$ .

Varian ProMALDI  
File: W04\_MALDI.trans

Mode: Positive  
Scans: 1  
Date: 29-SEP-2019  
Time: 15:38:25  
Scale: 29.3402





**Fig. S13.** HR-MS spectrum of compound 5T-2C8-Cl.

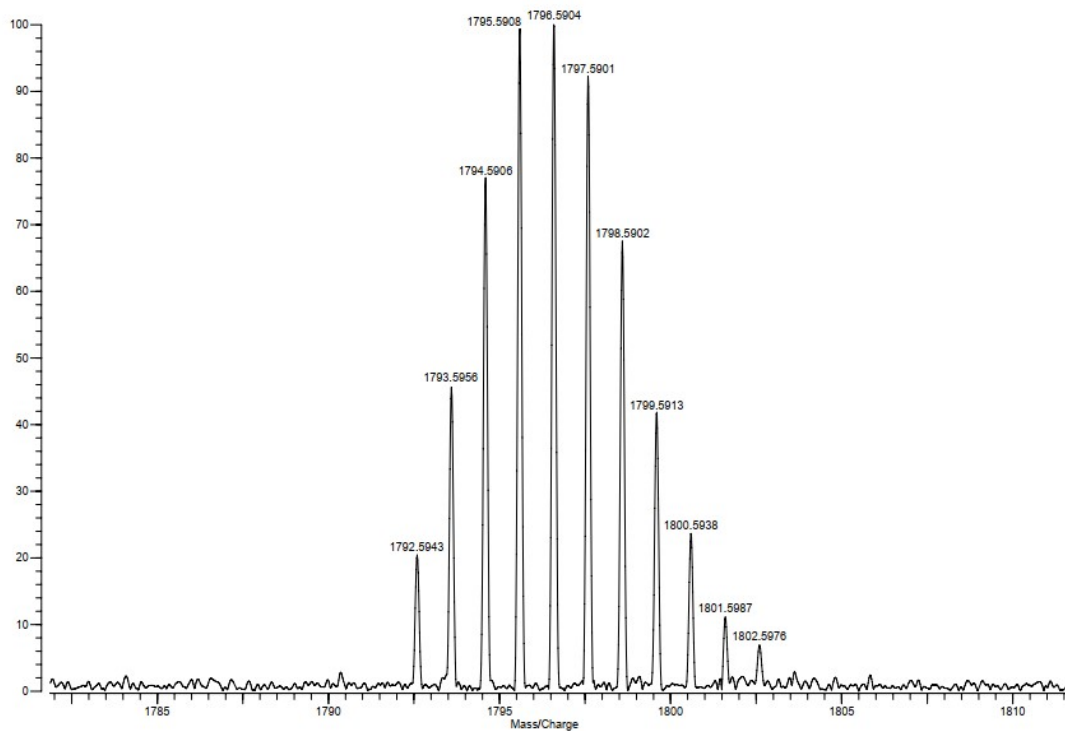


**Fig. S14.** HR-MS spectrum of compound 5T-2C8-2Cl.